








## Application the Galileo high accuracy service for unmanned aerial vehicles positioning in aerial navigation

Klaudia Cybulska-Gac<sup>1\*</sup>, Kamil Krasuski<sup>1</sup>, Robert Bąbel<sup>2</sup>,  
Stepan Savchuk<sup>1</sup>, Piotr Miduch<sup>1</sup>, Maciej Smolak<sup>3</sup>, Paweł Przybyłek<sup>2</sup>

<sup>1</sup> Faculty of Navigation and Logistic, Polish Air Force University, ul. Dywizjonu 303 nr 35, 08-521 Dęblin, Poland

<sup>2</sup> Faculty of Aviation, Polish Air Force University, ul. Dywizjonu 303 nr 35, 08-521 Dęblin, Poland

<sup>3</sup> Unmanned Aerial Vehicle Training Center, Polish Air Force University, ul. Dywizjonu 303 nr 35, 08-521 Dęblin, Poland

\* Corresponding author's e-mail: [k.cybulska-gac@law.mil.pl](mailto:k.cybulska-gac@law.mil.pl)

### ABSTRACT

The Galileo HAS (high accuracy system) service can be used in various modes of transport, including air, sea, and road. In the context of air navigation, its potential application in determining the position of aircraft or UAVs (unmanned aerial vehicles) during flight is of particular importance. The main objective of this work was to determine the accuracy of kinematic positioning of UAVs using HAS corrections in the context of air navigation in the field of transport. To achieve this objective, the position of the UAV was determined using the GPS/Galileo code observations and HAS corrections, and the accuracy of the determined BLH ellipsoidal coordinates of the UAV position in flight was determined. The aerial research used a DJI Matrice 350 UAV with a Septentrio Mosaic-X5 geodetic receiver installed on the platform with a module for recording HAS corrections in real time in SSR (State Space Representation) format. The calculations were performed using the RTKLIB program, which used GPS and Galileo navigation messages, GPS and Galileo code observations in RINEX format from the Septentrio Mosaic-X5 receiver, and HAS corrections converted to RTCM (Radio Technical Commission for Maritime) format. In turn, Emlid Studio v.1.9 software was used to determine the precise flight reference trajectory using the DD (Double Difference) phase solution. The accuracy analysis shows that the RMS errors for the HAS solution in SPP method are: 0.36 m for the B component, 1.49 m for the L component, and 8.36 m for the h component. The results of the study show the enormous potential of using the HAS service in air navigation. In the future, there are plans to conduct further research using HAS in UAV flights.

**Keywords:** UAV, Galileo, GPS, HAS, accuracy.

### INTRODUCTION

The Galileo navigation system was officially certified by ICAO for aviation applications in transport since the turn of 2023/2024 [1]. This allows it to be used in aviation operations, particularly in air navigation. Furthermore, the Galileo system had to meet specific GNSS positioning quality criteria in order to be approved for full operation in air transport. These criteria are accuracy, availability, and continuity [2]. These are the basic satellite positioning qualities that apply to global GNSS systems, such as GPS, GLONASS, Galileo, and BeiDou [1,

3]. For the Galileo system, the basic measures of satellite positioning quality in air transport are [1]:

- horizontal positioning accuracy for LNAV (Lateral Navigation) navigation should be between 5 m and 10 m with a probability of 95% throughout the entire flight,
- vertical positioning accuracy for VNAV (Vertical Navigation) navigation should be between 8 m and 16 m with a probability of 95% throughout the entire flight,
- Galileo positioning availability in the horizontal and vertical planes should be higher than 99% throughout the entire flight,

- the continuity of Galileo positioning must not exceed the value 1–4× per hour.

Therefore, owing to its navigation capabilities, the Galileo system can be used for kinematic positioning during flight tests. For air navigation, the key factors are the determined position and the accuracy of the determined coordinates of the user's position in flight. As shown by ICAO recommendations, C/A code observations on the E1 frequency [4] should be used to determine the kinematic position of Galileo in flight as part of the SPP method [5]. In addition, the data from the Galileo navigation message should be used in calculations to determine, for example, the satellite position, satellite clock error, ionospheric correction, relativistic effect, hardware delay for the satellite, etc. [6].

## THE STATE OF KNOWLEDGE

The Galileo code positioning using the SPP method can be corrected using the data from the HAS service. The HAS service allows corrections to be made to: satellite position, satellite clock error, and hardware delays to pseudo-range. The HAS positioning service transmits corrections in real time to the user using the E6 carrier frequency [7] and via the Internet as RTCM format. Owing to its dual availability, the HAS service also offers redundancy, increasing availability for aviation. The service operates 24 hours a day, 7 days a week, and is a free service of the Galileo system. The corrections transmitted can be used in both the Galileo and GPS navigation systems [8]. In addition, HAS corrections will ultimately be used in the PPP (Precise Point Positioning) positioning method [9, 10], although they will also be used in the SPP code method. The HAS service will provide corrections for the Galileo system on the E1/E5a/E5b/E6 frequencies and, accordingly, in the GPS- L1/L2/L5 system. At the current stage, the HAS service is operationally at level 1 and will ultimately be at level 2 [11, 12].

Currently, the HAS service is mainly used in geodetic surveys, supporting the improvement of the accuracy of precise satellite positioning using the PPP method [13, 14]. However, in line with the subject matter of this paper, the HAS service can be used in SPP code positioning for air navigation purposes. As shown in the literature, the SPP code method using Galileo HAS corrections has been used primarily in static GNSS measurements.

Thus, in [15, 16], the possibilities of using Galileo HAS corrections in SPP code positioning to increase the accuracy of the user's position determination were demonstrated. The article [17] compared the positioning accuracy, number of satellites, number of observations, and GDOP (Geometric DOP) coefficients between the SPP and PPP HAS solutions for the GPS and Galileo systems. The publication [18] showed the results of static positioning using HAS corrections for both the PPP and SPP methods. In the case of absolute SPP positioning, different configurations of solutions with GPS and Galileo observations at all carrier frequencies were presented. In article [19], the coordinates of selected IGS (International GNSS Service) reference stations were determined using the HAS service as part of SPP positioning. The accuracy of SPP positioning was higher than 3 m.

Another study [20] presented the results of dynamic SPP positioning with HAS corrections. In this case, the accuracy of SPP positioning in 3D space was approximately 7 m. Subsequent articles [21–23] compared the SPP code solution with PPP HAS. While the positioning accuracy of SPP is 3–4 m, after PPP HAS correction, the accuracy of coordinate determination increases to approximately 0.1 m. In article [24], HAS correction was used to determine the positioning accuracy of SPP for different types of GNSS receivers. The tests were performed for different configurations, calculation strategies, and carrier frequencies for the GPS and Galileo systems. On the basis of a review of the literature, it can be concluded that:

- the primary purpose of the HAS service is precise PPP positioning [13–24],
- the HAS service can also be used in absolute SPP positioning [15–24],
- Galileo HAS corrections were mainly used in static SPP positioning [15–24],
- in the case of kinematic positioning, the SPP HAS solution was used in [20] for car navigation.

## RESEARCH PROBLEM

Looking at the application of HAS corrections in the SPP absolute solution, one can mainly see the results of GNSS static positioning tests, which is characteristic of satellite surveying. However, for air navigation, and in particular air transport, kinematic solutions are needed during flight tests of aircraft or, for example, UAVs. This is very

important for ensuring and maintaining the continuity and availability of the Galileo and GPS signals in air navigation. Therefore, application solutions supported by research and the use of HAS corrections in kinematic positioning in aviation are necessary. This will allow for the verification of the use of the HAS service in air navigation in air transport. The main objective of the work was to determine the accuracy of UAV kinematic positioning using HAS corrections in air navigation in the field of transport. For this purpose, the position of the UAV was determined using GPS/Galileo code observations and HAS corrections, and the accuracy of the determined BLh ellipsoidal coordinates of the UAV position in flight was determined. The most important contributions of the author to this publication include:

- development of a GPS/Galileo positioning algorithm with HAS corrections,
- determination of HAS corrections during a UAV test flight,
- development of a computational strategy for determining the kinematic position of a UAV based on the SPP solution,
- determination of the accuracy of GPS/Galileo + HAS kinematic positioning in air transport,
- presentation of the results of PPP HAS kinematic positioning in air navigation.

The work was divided into the following chapters: 1) Introduction, 2) analysis of state of the knowledge, 3) Research problem, 4) Materials and methods, 5) Research results, 6) Discussion, 7) Conclusions.

## MATERIALS AND METHODS

As it was mentioned in the introduction, HAS corrections can be used for both Galileo and GPS measurements. Therefore, the basic observation equation for SPP GPS/Galileo positioning with HAS corrections will take the form (Eq. 1) [24, 25]:

$$\begin{cases} l_{Gal,HAS} = d_{Gal,HAS} + c \cdot (dtr_{Gal} - dts_{Gal,HAS}) + Ion_{Gal} + Trop_{Gal} + Rel_{Gal} + GGD \\ l_{GPS,HAS} = d_{GPS,HAS} + c \cdot (dtr_{GPS} - dts_{GPS,HAS}) + Ion_{GPS} + Trop_{GPS} + Rel_{GPS} + TGD \end{cases} \quad (1)$$

$$\begin{cases} d_{Gal,HAS} = \sqrt{(X_r - X_{Gal,HAS})^2 + (Y_r - Y_{Gal,HAS})^2 + (Z_r - Z_{Gal,HAS})^2} \\ d_{GPS,HAS} = \sqrt{(X_r - X_{GPS,HAS})^2 + (Y_r - Y_{GPS,HAS})^2 + (Z_r - Z_{GPS,HAS})^2} \end{cases} \quad (3)$$

where:  $l_{Gal,HAS}$  – pseudorange in Galileo measurements, corrected by HAS corrections,  $l_{GPS,HAS}$  – pseudorange in GPS measurements, corrected by HAS corrections,  $d_{Gal,HAS}$  – geometric distance in Galileo measurements, corrected by HAS corrections,  $d_{GPS,HAS}$  – geometric distance in GPS measurements, corrected by HAS corrections,  $c$  – speed of light, constant value,  $dtr_{Gal}$  – receiver clock error in Galileo measurements,  $dtr_{GPS}$  – receiver clock error in GPS measurements,  $dts_{Gal,HAS}$  – satellite clock error in Galileo measurements, corrected by HAS corrections,  $dts_{GPS,HAS}$  – satellite clock error in GPS measurements, corrected by HAS corrections,  $Ion_{Gal}$  – ionospheric correction in Galileo measurements,  $Ion_{GPS}$  – ionospheric correction in GPS measurements,  $T_{ropGal}$  – tropospheric correction in Galileo measurements,  $T_{ropGPS}$  – tropospheric correction in GPS measurements,  $Rel_{Gal}$  – relativistic correction in Galileo measurements,  $Rel_{GPS}$  – relativistic correction in GPS measurements,  $GGD$  – instrumental biases for satellites in Galileo measurements,  $TGD$  – instrumental biases for satellites in GPS measurements.

In Equation 1, three parameters are corrected by HAS corrections, i.e., pseudorange, geometric distance, and satellite clock error. Therefore, it can be written that the pseudorange parameter is [24]:

$$\begin{cases} l_{Gal,HAS} = l_{Gal} + \delta l_{HAS} \\ l_{GPS,HAS} = l_{GPS} + \delta l_{HAS} \end{cases} \quad (2)$$

where:  $l_{Gal}$  – pseudorange in Galileo measurements,  $l_{GPS}$  – pseudorange in GPS measurements,  $\delta l_{HAS}$  – HAS corrections to pseudorange.

Then, the geometric distance parameter is expressed as (Eq. 3):

where:  $(X_r, Y_r, Z_r)$  – receiver antenna coordinates, user position determined,  $X_{Gal,HAS}$  – X coordinate of the Galileo satellite position after HAS correction,  $Y_{Gal,HAS}$  – Y coordinate of the Galileo satellite position after HAS correction,  $Z_{Gal,HAS}$  – Z coordinate of the Galileo satellite position after HAS correction,  $X_{GPS,HAS}$  – X coordinate of the GPS satellite position after HAS correction,  $Y_{GPS,HAS}$  – Y coordinate of the GPS satellite position after HAS correction,  $Z_{GPS,HAS}$  – Z coordinate of the GPS satellite position after HAS correction.

Accordingly, the HAS correction for individual XYZ coordinates of GPS and Galileo satellites is as follows [24]:

- for Galileo satellites:

$$\begin{cases} X_{Gal,HAS} = X_{Gal} + \delta X \\ Y_{Gal,HAS} = Y_{Gal} + \delta Y \\ Z_{Gal,HAS} = Z_{Gal} + \delta Z \end{cases} \quad (4)$$

- for GPS satellites:

$$\begin{cases} X_{GPS,HAS} = X_{GPS} + \delta X \\ Y_{GPS,HAS} = Y_{GPS} + \delta Y \\ Z_{GPS,HAS} = Z_{GPS} + \delta Z \end{cases} \quad (5)$$

where:  $X_{Gal}$  – X coordinate of the Galileo satellite position from the navigation message,  $Y_{Gal}$  – Y coordinate of the Galileo satellite position from the navigation message,  $Z_{Gal}$  – Z coordinate of the Galileo satellite position from the navigation message,  $X_{GPS}$  – X coordinate of the GPS satellite position from the navigation message,  $Y_{GPS}$  – Y coordinate of the GPS satellite position from the navigation message,  $Z_{GPS}$  – Z coordinate of the GPS satellite position from the navigation message,  $(\delta X, \delta Y, \delta Z)$  – HAS orbit correction.

Finally, the orbit correction parameters  $(\delta X, \delta Y, \delta Z)$  taking into account HAS corrections are calculated as [26, 27]:

$$\begin{cases} \delta X = e_R \cdot \delta R \\ \delta Y = e_A \cdot \delta A \\ \delta Z = e_C \cdot \delta C \end{cases} \quad (6)$$

where:  $e_R, e_A, e_C$  – unit vectors in the radial, along, and cross directions,  $\delta R, \delta A, \delta C$  – orbit correction vector in the radial, along, and cross directions.

The satellite clock error based on HAS correction is calculated as [28, 29]:

$$\begin{cases} dts_{Gal,HAS} = dts_{Gal} + \frac{\delta dts_{HAS}}{c} \\ dts_{GPS,HAS} = dts_{GPS} + \frac{\delta dts_{HAS}}{c} \end{cases} \quad (7)$$

where:  $dts_{Gal}$  – Galileo satellite clock error from navigation message,  $dts_{GPS}$  – GPS satellite clock error from navigation message,  $\delta dts_{HAS}$  – HAS correction for satellite clock error.

On the basis of on Equations 1–7, the unknown coordinates of the receiver  $(X_r, Y_r, Z_r)$  [30] and the errors of the receiver clocks ( $dtr_{Gal}, dtr_{GPS}$ ) in the Galileo and GPS systems will be determined in the SPP positioning process [31]. The unknown parameters  $(X_r, Y_r, Z_r, dtr_{Gal}, dtr_{GPS})$  will be determined by the least squares method using a system of normal equations in a sequential process for a given measurement epoch [5, 32]. The determined coordinates of the user’s position  $(X_r, Y_r, Z_r)$  in accordance with the ICAO recommendations are presented and expressed using BLh geodetic coordinates in the form of geodetic latitude, geodetic longitude, and ellipsoidal height [33]. For this purpose, Helmert’s formulas are used to transform geocentric XYZ coordinates into geodetic BLh coordinates [34]. And now, on this basis, the BLh coordinates will determine the user’s position.

The developed algorithm (1-7) was used in experimental flight tests using a UAV. A DJI Matrice 350 UAV with a built-in GNSS RTK precision positioning module was used in the flight test [35]. A Septentrio Mosaic-X5 surveying receiver with a real-time HAS correction recording module [36] recording module in real time in SSR format [37]. The Septentrio Mosaic-X5 receiver is a multi-system and multi-frequency GNSS receiver. For the purposes of the research, the GNSS receiver collected the GPS and Galileo observations and HAS corrections in real time during the flight. The built-in Septentrio Mosaic-X5 receiver on the UAV platform is shown in Figure 1.

The test flight of the unmanned platform took place on April 7<sup>th</sup>, 2025, between 10:22:47 and 10:41:50 GPST. The final destination of the experiment was the town of Sobieszyn in the Ryki County, as shown in Figure 2.

The collected GNSS data and HAS corrections allowed the position of the UAV to be determined according to a set of mathematical



Figure 1. The UAV with Septentrio Mosaic-X5 receiver before flight experiment

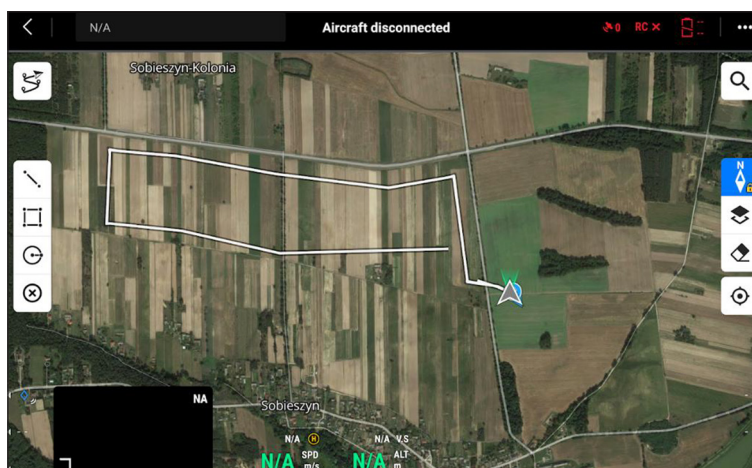


Figure 2. The designed flight path of the UAV

equations (1-7). The calculations were performed using RTKLIB v.2.4.3 software [38], in which the UAV coordinates were determined from the SPP GPS/Galileo solution with HAS corrections [39]. The following calculation configuration was set in the RTKLIB software [40]:

- positioning method: SPP code method,
- observation type: code on frequencies L1 (GPS), E1 (Galileo),
- elevation mask:  $5^\circ$ ,
- ionosphere correction: based on GPS and Galileo navigation messages,
- troposphere correction: Saastamoinen model,
- orbit model: based on GPS and Galileo navigation messages + HAS correction,
- satellite clock error: based on GPS and Galileo navigation messages + HAS correction,

- GNSS system: GPS + Galileo,
- calculation interval: 1 s,
- maximum DOP value [41]: 30,
- final position coordinates: BLh geodetic coordinates,
- receiver antenna phase center: based on ANTEX file from IGS [42].

The calculations in RTKLIB used the GPS and Galileo navigation messages, GPS and Galileo code observations in RINEX format from a Septentrio Mosaic-X5 receiver, and HAS corrections converted to RTCM format. In turn, Emlid Studio v.1.9 [43] software, the precise flight reference trajectory was determined using the DD (Double Difference) solution [44]. The calculations used GPS and Galileo navigation messages, GPS and Galileo code observations in RINEX

format from the Septentrio Mosaic-X5 receiver, and GNSS observations in RINEX format from the RYKI reference station of the ASG-EUSPOS system [45]. Next, a proprietary numerical script written in Scilab 6.1.1 [46] was used in the calculations to determine the relevant UAV positioning accuracy parameters in accordance with the objective of the study. First, position errors [47] were calculated according to formula (8):

$$\begin{cases} \Delta B = B_r - B_{ref} \\ \Delta L = L_r - L_{ref} \\ \Delta h = h_r - h_{ref} \end{cases} \quad (8)$$

where:  $(\Delta B, \Delta L, \Delta h)$  – positioning errors of the SPP GPS/Galileo + HAS solution,  $B_r, L_r, h_r$  – obtained coordinates of the UAV vehicle based on transformation between XYZ geocentric coordinates and BLh geodetic coordinates,  $(B_{ref}, L_{ref}, h_{ref})$  – reference coordinates of the UAV vehicle based on DD solution.

Finally, the root mean square errors were also calculated according to Equation 9 [48]:

$$\begin{cases} RMS\Delta B = \sqrt{\frac{[\Delta B^2]}{N}} \\ RMS\Delta L = \sqrt{\frac{[\Delta L^2]}{N}} \\ RMS\Delta h = \sqrt{\frac{[\Delta h^2]}{N}} \end{cases} \quad (9)$$

where:  $RMS\Delta B, RMS\Delta L, RMS\Delta h$  – RMS error for BLh coordinates,  $N$  – number of observations.

The entire research methodology is shown in a block diagram in Figure 3. The calculation process is multi-stage, as it begins with a UAV flight and the collection of the GNSS data in real time by the on-board receiver, followed by the determination of the UAV coordinates according to Equations 1–7, by reconstructing the precise reference trajectory of the UAV flight, and finally by determining the positioning accuracy of the UAV for the proposed research methodology. The obtained research results were presented in the next two chapters of the article.

## RESEARCH RESULTS

The research results first show the number of tracked GPS+Galileo satellites with HAS

corrections, as shown in Figure 4. As it can be seen, the number of the GPS+Galileo satellites with HAS solution ranges from 11 to 14. The largest number of the GPS+Galileo satellites with the solution is visible in the final phase of the UAV flight. Figures 5 and 6 show individual GPS and Galileo satellites with HAS corrections during the UAV flight. In the case of the GPS system, satellites G05, G16, G20, G23, G26, G28, G29, and G31 were tracked. In the case of the GPS system, satellites E05, E13, E15, E21, E23, E26, E31, and E33 were tracked.

Table 1 shows the distribution of HAS corrections for the GPS and Galileo satellites. In the case of satellite clock error corrections, the values of the parameter  $\delta dt_{s_{HAS}}$  range from -1.925 m to 1.053 m for the GPS satellites and from -0.267 m to 0.422 m for the Galileo satellites. Furthermore, for HAS orbit corrections, the parameter values ( $\delta R, \delta A, \delta C$ ) range from -2.376 m to 0.960 m for the GPS satellites and from -0.608 m to 0.392 m for the Galileo satellites. In turn, for code measurement error correction, the values of the  $\delta l_{HAS}$  parameter are as follows: from -3.520 m to 2.080 m for the GPS satellites, and from -1.840 m to 1.700 m for the Galileo satellites. Both in the case of parameters

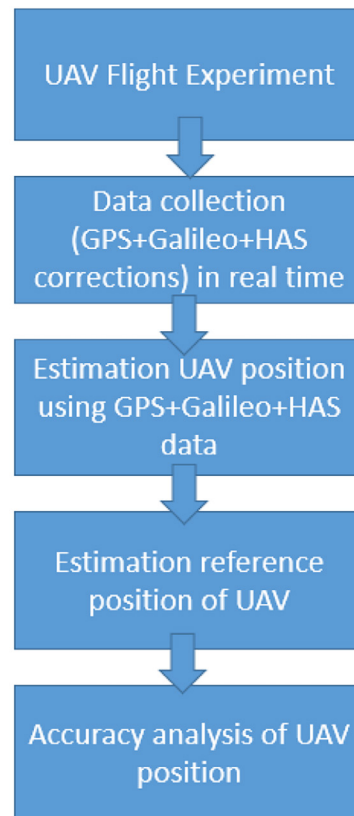


Figure 3. The flowchart of the research method

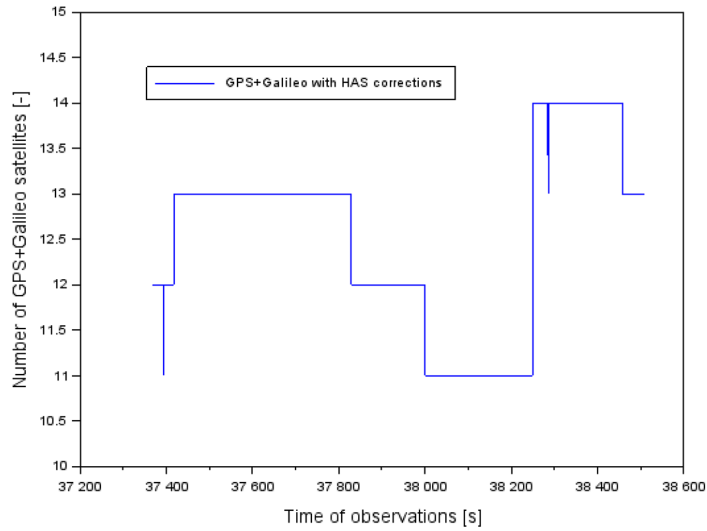


Figure 4. Number of the GPS+Galileo satellites with HAS corrections

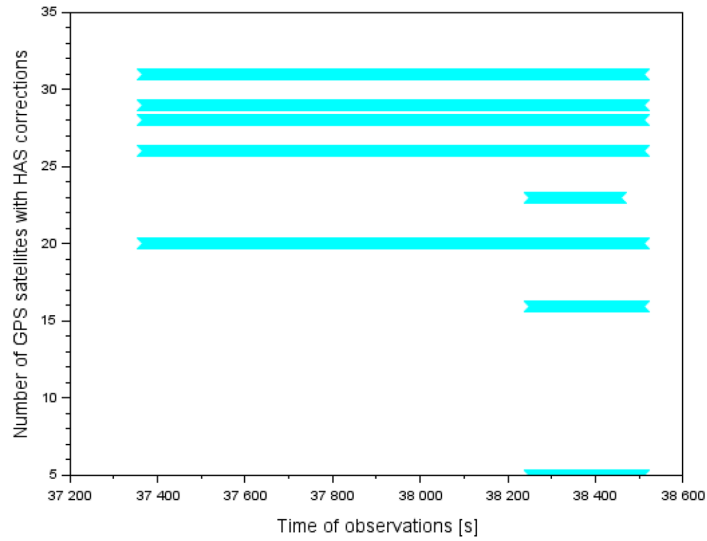


Figure 5. Number of the GPS satellites with HAS corrections

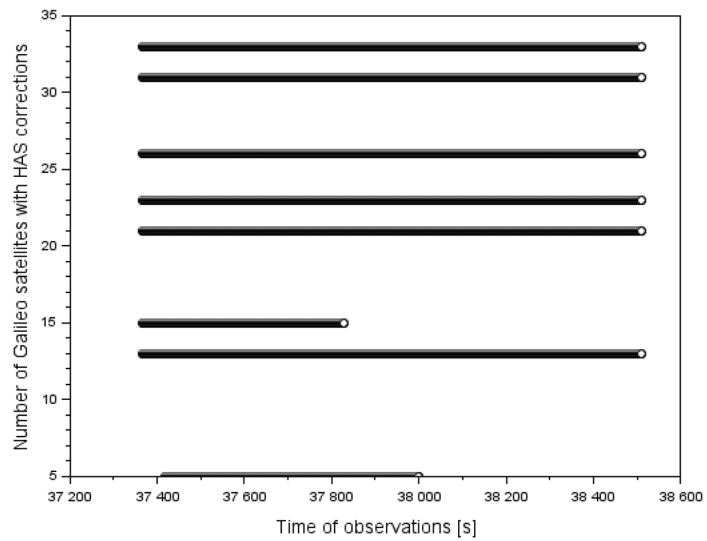


Figure 6. Number of the Galileo satellites with HAS corrections

**Table 1.** The HAS corrections for the GPS and Galileo satellites

Satellite ID	clock satellite correction [m]	$(\delta R, \delta A, \delta C)$ orbit satellite correction [m]	$\delta I_{HAS}$ code bias correction [m]
G05	from 0.790 to 1.053	from -0.544 to 0.168	0.920
G16	from -0.967 to -0.775	from 0.065 to 0.960	2.080
G20	from -1.925 to -1.515	from -0.135 to 0.632	1.820
G23	from -0.090 to -0.008	from -1.072 to 0.400	0.360
G26	from -0.622 to -0.283	from -0.040 to 0.480	-3.520
G28	from -0.162 to 0.192	from -2.376 to 0.135	1.000
G29	from -0.160 to 0.170	from -0.576 to 0.632	0.800
G31	from -0.232 to 0.160	from -0.408 to 0.230	2.040
E05	from -0.172 to -0.087	from -0.352 to 0.112	-1.100
E13	from 0.057 to 0.125	from -0.512 to 0.160	1.700
E15	from -0.265 to -0.197	from -0.088 to 0.097	-1.840
E21	from 0.282 to 0.335	from -0.248 to 0.048	-0.720
E23	from -0.267 to -0.180	from -0.120 to -0.024	-0.460
E26	from 0.287 to 0.357	from -0.608 to 0.392	1.220
E31	from -0.135 to -0.012	from -0.232 to -0.055	-1.360
E33	from 0.335 to 0.422	from -0.152 to 0.296	1.040

$(\delta R, \delta A, \delta C)$  and the parameter  $\delta I_{HAS}$  it is clear that the greater dispersion of HAS corrections is visible in the GPS system than in Galileo. It can be concluded that HAS corrections are better suited to the Galileo satellites than GPS. Figure 7 shows the positioning errors ( $\Delta B, \Delta L, \Delta h$ ) determined from mathematical Equation 8. The positioning errors ( $\Delta B, \Delta L, \Delta h$ ) were as follows:

- from -1.05 m to 0.52 m for coordinate B,
- from 0.90 m to 2.16 m for coordinate L,
- from -9.64 m to -6.37 m for coordinate h.

In addition, the arithmetic mean values for the parameters ( $\Delta B, \Delta L, \Delta h$ ) are equal to: -0.27 m for coordinate B, 1.47 m for coordinate L, -8.35 m for coordinate h. On the basis of the results ( $\Delta B, \Delta L, \Delta h$ ) it can be concluded that the accuracy of the horizontal coordinates is higher than the accuracy of the ellipsoidal height h. Furthermore, the RMS errors determined from equation (9) are: 0.36 m for the B component, 1.49 m for the L component, and 8.36 m for the h component. For horizontal BL components, the positioning accuracy of the UAV is relatively high, with a maximum of  $\pm 2.16$  m. This is much better than the theoretical accuracy recommended by ICAO [1]. Therefore, the impact of HAS correction is positive for LNAV horizontal navigation. The situation is completely different when it comes to the accuracy of the ellipsoidal height h. Here, the results are much worse than for the horizontal components

BL. However, the results for the accuracy of the ellipsoidal height h are within the ICAO technical recommendations for the Galileo system [1].

## DISCUSSION

The discussion of the research results obtained was divided into seven parts, i.e.,

- study of the impact of navigation messages on positioning accuracy,
- comparison of the research results obtained with the classic SPP GPS/Galileo solution,
- modification of the calculation strategy of the SPP GPS/Galileo + HAS solution,
- verification of the research methodology in a second independent aviation experiment,
- application of HAS corrections in the PPP measurement technique and determination of the accuracy of PPP HAS positioning,
- comparison of the PPP HAS research results obtained with IGS products,
- and comparison of the research results obtained with the analysis of the state of knowledge.

### The impact of navigation messages on positioning accuracy

The first considerations in the discussion concern determining the impact of ephemeris data on the positioning accuracy of UAVs. In this regard,

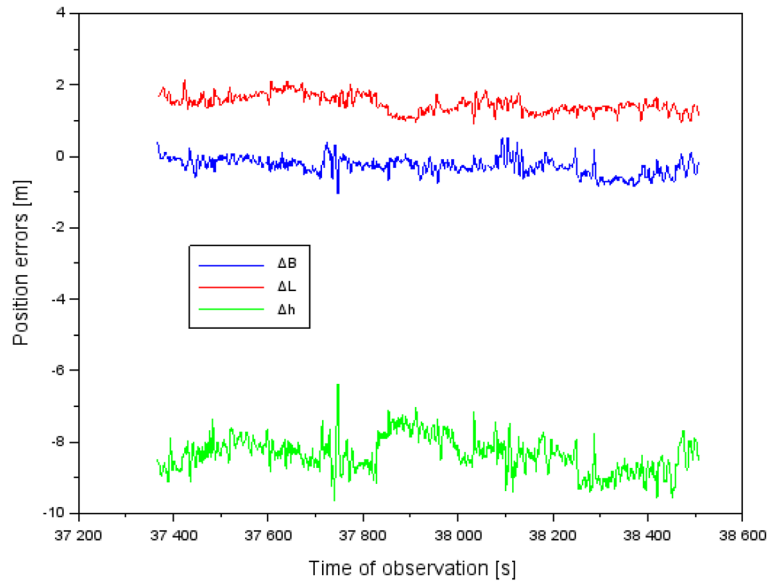


**Figure 7.** Position errors for the BLh coordinates based on the GPS/Galileo + HAS solution

it was checked whether changing the navigation message would affect the positioning accuracy of UAVs in any way. For the calculations, a daily navigation message was used, recorded by the Trimble NETR9 GNSS receiver [49] located at the BOR1 reference station belonging to the IGS network [50]. The calculation strategy remained unchanged, and the calculations were performed using the RTKLIB program. In this case, the number of the GPS+Galileo satellites with HAS corrections ranged from 12 to 15. Therefore, the quality of ephemeris data and satellite configuration also affect the determination of the UAV’s kinematic

position. Figure 8 shows the results of position errors after changing the navigation message. It is worth noting that the positioning accuracy of the UAV has changed. The position errors ranged from -0.26 m to 1.02 m for the B component, from 0.63 m to 1.81 m for the L component, and from -7.94 m to -5.59 m for the h component. While for the horizontal BL components the RMS error reached approximately 0.42 m and 1.19 m, respectively, the results for the ellipsoidal height h accuracy are very interesting. The RMS error value for this component is now 6.95 m. And now, comparing the results from Figures 7 and 8 for the h coordinate,

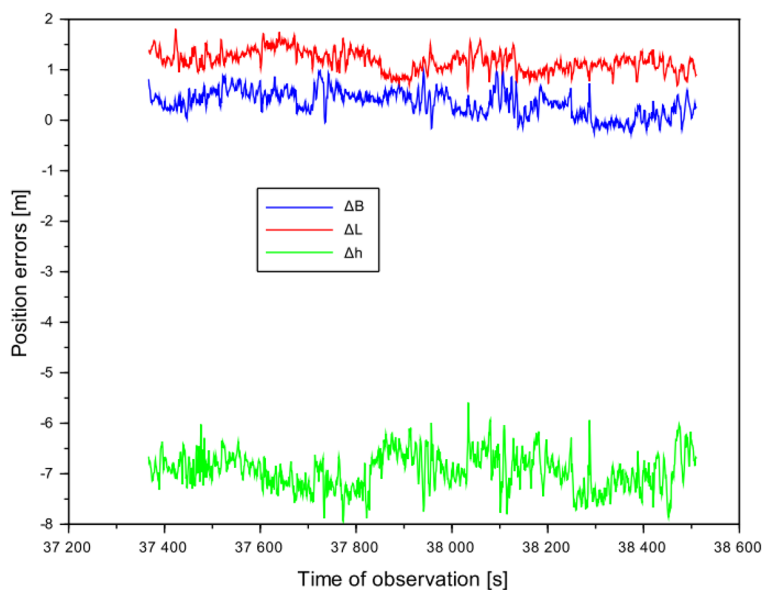


**Figure 8.** Position errors for the BLh coordinates based on GPS/Galileo + HAS solution after modification the navigation message

the accuracy has been improved by 17%. The RMS error difference for vertical height  $h$  is 1.41 m. This is extremely important in the context of improving flight safety in the VNAV vertical plane. Therefore, the quality of ephemeris data also appears to be crucial in the kinematic positioning of UAVs.

### Comparison the SPP GPS/Galileo + HAS corrections vs. classic SPP GPS/Galileo solution

In the second part of the discussion, the positioning accuracies obtained were compared with the classic SPP GPS/Galileo solution [51]. Figure 9 shows the position errors for the classic SPP GPS/Galileo solution. The position errors range from -1.51 m to -0.03 m for the B component, from 1.30 m to 2.34 m for the L component, and from -10.19 m to -6.81 m for the h component. In addition, the RMS errors are equal to: 0.78 m for the B coordinate, 1.84 m for the L coordinate, and 8.60 m for the h coordinate. Now, comparing the positioning accuracy results in the form of RMS errors from the SPP GPS/Galileo + HAS solution and SPP GPS/Galileo alone, it can be seen that:

- the RMS error for the B component in the SPP GPS/Galileo + HAS solution is 53% lower,
- the RMS error for the L component in the SPP GPS/Galileo + HAS solution is 19% lower,
- the RMS error for the h component in the SPP GPS/Galileo + HAS solution is 3% lower.

When compared with the results in Figure 8, it can be concluded that the change in the navigation

message resulted in an improvement in accuracy in terms of RMS errors for: component B by 46%, component L by 35%, and component  $h$  by 20%. Of particular interest is the improvement in the determination of the ellipsoidal height  $h$ . On this basis, it can be said that HAS correction improved the positioning of SPP GPS/Galileo for all three components of the BLh position. Therefore, its use in the SPP code method is justified.

### Modification of the calculation strategy involving the SPP GPS/Galileo + HAS solution

The third part of the discussion was devoted to the analysis of the computational strategy, with particular emphasis on the impact of the elevation angle on the positioning accuracy of SPP GPS/Galileo with HAS corrections. Table 2 shows the results of the impact of elevation angle truncation on the accuracy of UAV kinematic positioning. The configuration for recording GPS/Galileo code observations by the GNSS receiver was selected at  $5^\circ$  and  $10^\circ$ , respectively, and then the positioning accuracy was calculated in the form of RMS errors. While the elevation angle cut-off of  $5^\circ$  is imposed by ICAO [1], such code observations are subject to high measurement noise [52]. Increasing the elevation angle cut-off reduces measurement noise and the multipath effect [53], thus affecting the quality of the position navigation solution. Table 2 shows that increasing the elevation angle cutoff can improve the position navigation solution and increase the accuracy of UAV

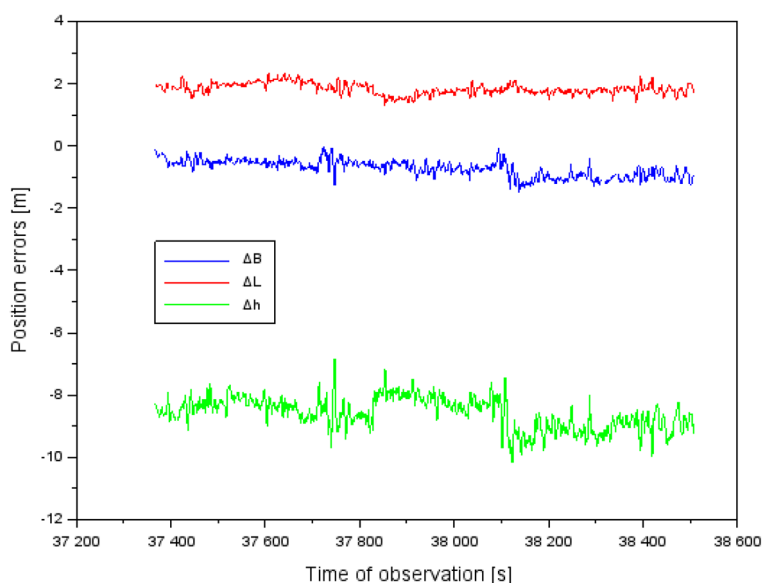


Figure 9. Position errors for the BLh coordinates based on the GPS/Galileo solution

kinematic positioning. The positioning accuracy results presented in Table 2 vary within the range of  $\pm 0.11$ – $0.25$  m. On the other hand, it should not be forgotten that increasing the elevation angle cut-off eliminates some GPS/Galileo satellites from the position navigation solution [54].

**Verification of the research methodology in a second aviation experiment**

The next part of the discussion will present the results of accuracy tests in another independent aerial experiment using a UAV. This time, the flight was performed on July 25<sup>th</sup>, 2025, also in the Ryki district. The calculation strategy, configuration settings, software used, unmanned platform, and GNSS receiver were the same as described in the “Materials and methods” section. It is worth noting that the number of tracked GPS+Galileo satellites changed, as shown in Figure 10. In the second experiment, the number of GPS/Galileo satellites with HAS corrections ranged from 5 to 21. This translated into the quality of the determined

UAV position coordinates and the accuracy itself, as shown in Figure 11. The position errors in the second UAV flight ranged from  $-0.11$  m to  $2.03$  m for the B component, from  $1.09$  m to  $2.10$  m for the L component, and from  $-2.49$  m to  $1.51$  m. In addition, the RMS errors are equal to:  $0.53$  m,  $1.62$  m,  $1.63$  m for individual BLh coordinates. It is now clear that the number of GPS/Galileo satellites is of great importance when analyzing the accuracy of UAV kinematic positioning. In addition, the positioning accuracy results in the second UAV flight are better than in flight no. 1.

**Comparison of the PPP HAS solution vs. reference position**

The fifth part of the discussion concerns the possibility of applying HAS corrections in the PPP measurement technology and determining the positioning accuracy of PPP HAS for the UAV technology [55]. Figure 12 shows the results of position errors for PPP HAS positioning in dynamic mode for UAVs. The PPP HAS solution was implemented in RTKLIB v.2.4.3 [40] for the GPS/Galileo data from flight test no. 1. The position errors from the calculations were as follows: from  $0.08$  m to  $0.94$  m for the B component, from  $0.44$  m to  $1.71$  m for the L component, and from  $-1.82$  m to  $-0.08$  m for the h component. The RMS errors are as follows:  $0.77$  m for the B coordinate,  $0.59$  m for the L coordinate, and  $0.48$  m for the h coordinate. In the case of the PPP measurement technique, the results obtained are

**Table 2.** The impact of cut off elevation in positioning accuracy analysis

Cut off elevation	Positioning accuracy [m]
5°	RMS $\Delta$ B = 0.36 m RMS $\Delta$ L = 1.49 RMS $\Delta$ h = 8.36
10°	RMS $\Delta$ B = 0.25 RMS $\Delta$ L = 1.33 RMS $\Delta$ h = 8.11

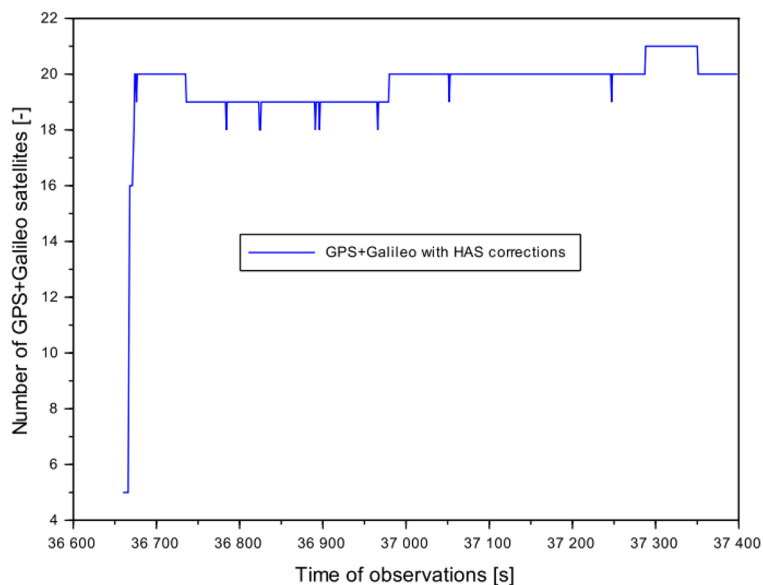


**Figure 10.** Number of the GPS+Galileo satellites with HAS corrections in the 2nd flight test

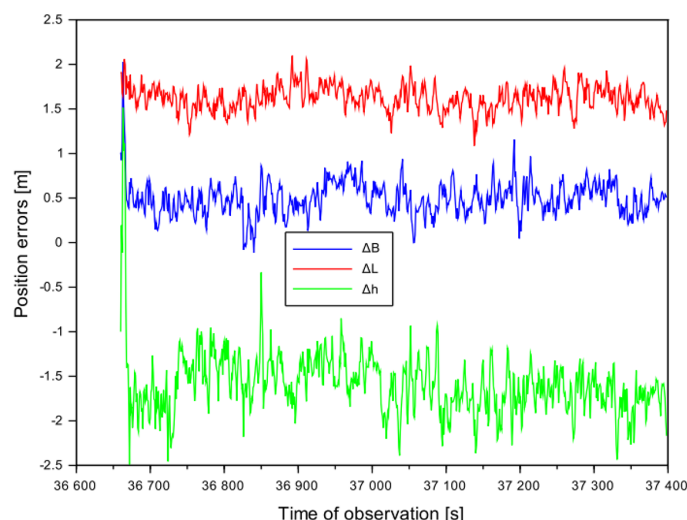


**Figure 11.** Position errors for the BLh coordinates based on the GPS/Galileo + HAS solution in the 2nd flight test

promising, as the target positioning accuracy of the HAS service for this method will be higher than 0.4 m [11, 12]. This will force changes in GNSS positioning in aviation, as the target accuracy will be higher than 1 m in real time owing to Galileo services. These changes will result in the installation of on-board GNSS receivers with the HAS service and coupling with the on-board avionics of an aircraft, including UAVs.

**Comparison of the PPP HAS solution vs. PPP IGS solution**

The sixth part of the discussion compares the positioning accuracy results of PPP HAS with the PPP solution based on IGS products [56]. For this purpose, the CSRS-PPP online service [57, 58] was used, which bases its PPP calculations on products from the EMR Analysis Center and other Analysis Centers within the IGS service [59]. The results of the BLh ellipsoidal coordinates from the PPP HAS solution and CSRS-PPP as the PPP solution with IGS products were compared. The difference in BLh coordinates was calculated from Equation 10 [60]:

$$\begin{cases} rB = B_{PPP\ HAS} - B_{CSRS-PPP} \\ rL = L_{PPP\ HAS} - L_{CSRS-PPP} \\ rh = h_{PPP\ HAS} - h_{CSRS-PPP} \end{cases} \quad (10)$$

where:  $rB, rL, rh$  – difference of coordinates between the PPP HAS and PPP IGS solutions,  $B_{PPP\ HAS}, L_{PPP\ HAS}, h_{PPP\ HAS}$  – the obtained coordinates of the UAV vehicle in flight test no. 1 based on the PPP HAS solution from the RTKLIB software,

$B_{CSRS-PPP}, L_{CSRS-PPP}, h_{CSRS-PPP}$  – the obtained coordinates of the UAV vehicle in flight test no. 1 based on the PPP IGS solution from the CSRS-PPP software.

Figure 13 presents the results of the difference in ellipsoidal coordinates of UAV positions between the PPP HAS and PPP IGS solutions. The values of the parameters ( $rB, rL, rh$ ) are as follows: from -0.48 m to 0.38 m along the B axis, from -0.31 m to 0.94 m along the L axis, and from -1.76 m to -0.05 m along the h axis. Additionally, the arithmetic mean of the parameter results ( $rB, rL, rh$ ) is: 0.17 m, -0.20 m, and -0.34 m for the individual BLh component. This shows a very good match between the results from the PPP HAS solution from the RTKLIB program and the PPP IGS from the CSRS-PPP program. The convergence time is approximately 200 s. After this time, the parameter results ( $rB, rL, rh$ ) stabilize until the end of the test.

**Comparison of the obtained results and methods vs. analysis of the state of knowledge**

The last part of the discussion compares the obtained research results with the current state of knowledge from the available literature. When analyzing the authorial contribution and the literature on the state of knowledge, it can be concluded that:

- the article determines the position of the UAV using Galileo HAS corrections, similarly to publication [55],
- Galileo HAS corrections were used in the SPP absolute positioning method [8, 15–24],

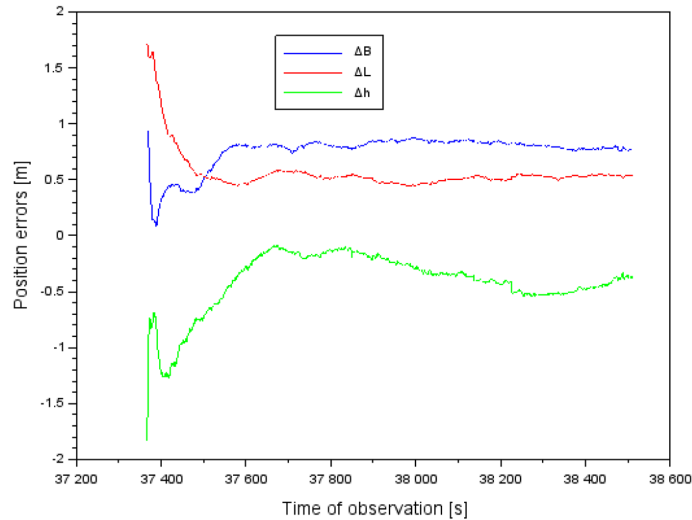


Figure 12. Position errors for the BLh coordinates based on the PPP HAS solution

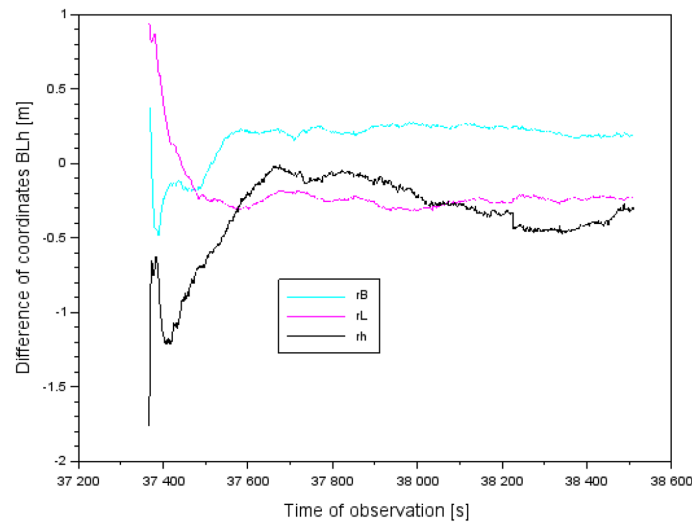


Figure 13. Difference of coordinates between the PPP HAS and PPP IGS solutions

- positioning accuracy was analyzed [8, 15–24],
- the article demonstrates the possibility of using the Galileo HAS service for the PPP measurement technique [13, 14, 36, 39, 55],
- the SPP GPS/Galileo + HAS positioning accuracy obtained during the research is similar to the results described in [19–24].

**CONCLUSIONS**

The main objective of the article was to determine the accuracy of UAV kinematic positioning using HAS corrections in the context of air navigation in the transport sector. The research and analyses conducted for this purpose confirmed that the use of HAS corrections in the SPP method for UAVs significantly improves positioning

accuracy. On the basis of the research conducted, it was demonstrated that:

1. HAS improves the accuracy of SPP code positioning:
  - the RMS error compared to the classic SPP solution was reduced by: 53% for the B component, 19% for the L component, and 3% for the h component,
  - when using a daily navigation message, it is possible to increase the accuracy of the vertical component h by up to 17%,
  - in the second UAV flight, positioning accuracy higher than 1.63 m was achieved for the BLh components.
2. The use of Galileo HAS measurement correction in the PPP technique in dynamic mode for UAVs allows for high positioning accuracy:

- the obtained RMS error values for the BLh geodetic components are at the level of: 0.77 m, 0.59 m, 0.48 m and confirm the effectiveness of this method.
3. The results of PPP HAS are consistent with the PPP solutions based on IGS products:
- the differences in BLh coordinates between PPP HAS and PPP IGS do not exceed 1 meter,
  - the arithmetic mean of the parameter results ( $rB$ ,  $rL$ ,  $rh$ ) is: 0.17 m, -0.20 m, and -0.34 m for each BLh component.

The research for the article was conducted in the Ryki district, in the vicinity of the Polish Air Force University in Dęblin. Therefore, although it was local in nature, its significance is enormous in terms of its potential use in the field of air navigation in transport. For the purposes of the article, two independent UAV flights were carried out to support the developed research methodology. As the literature shows, the HAS service had limited application in aviation, so the UAV flights and kinematic studies carried out can significantly contribute to the development of this correction service in the field of transport. Further research on the application of the HAS correction service in real-time kinematic positioning of UAVs is planned for the future. The research will be conducted with particular use of the HAS service for the development of air transport.

## REFERENCES

1. International Civil Aviation Organization. ICAO Standards and Recommended Practices (SARPS), 2006. Annex 10, Volume I (Radio Navigation Aids). Available from: <http://www.ulc.gov.pl/pl/prawo/prawomi%C4%99dzynarodowe/206-konwencje>. (Accessed: 01.06.2025).
2. Jafernik H., Krasuski K., Michta J. Assessment of suitability of radionavigation devices used in air. *Scientific Journal of Silesian University of Technology. Series Transport*. 2016, 90, 99–112, <https://doi.org/10.20858/sjsutst.2016.90.9>
3. Cybulska-Gac K., Krasuski K., Ciec ko A. Accuracy analysis of Galileo code positioning for UAV. *Scientific Journal of Silesian University of Technology. Series Transport*. 2025, 127, 39–55, <https://doi.org/10.20858/sjsutst.2025.127.3>
4. Robustelli U., Paziewski J., Pugliano G. Observation quality assessment and performance of GNSS stand-alone positioning with code pseudoranges of dual-frequency android smartphones. *Sensors*, 2021, 21, 2125, <https://doi.org/10.3390/s21062125>
5. Krasuski K., Aircraft positioning using SPP method in GPS system, *Aircraft Engineering and Aerospace Technology*, 2018, 90(8), 1213–1220, <https://doi.org/10.1108/AEAT-03-2017-0087>
6. Zhang J., Li W. Analysis of post-processed pseudorange-based point positioning with different data sources for the current galileo constellations. *Sensors* 2024, 24, 2472, <https://doi.org/10.3390/s24082472>
7. Naciri N., Yi D., Bisnath S., de Blas J., Capua R. Assessment of Galileo High Accuracy Service (HAS) test signals and preliminary positioning performance, *GPS Solutions*, 2023, 27 Article No. 73, Springer, 2023, <https://doi.org/10.1007/s10291-023-01410-y>
8. Gioia C., Borio D., Susi M., Fernandez-Hernandez I. The Galileo High Accuracy Service (HAS): Decoding and Processing Live Corrections for Code-Based Positioning, In *Proceedings of the 2022 International Technical Meeting of The Institute of Navigation*, Long Beach, California, January 2022, 1065–1074, <https://doi.org/10.33012/2022.18204>
9. Martini I., Susi M., Paonni M., Sgammini M., Fernandez-Hernandez I., Satellite Anomaly Detection with PPP Corrections: A case study with Galileo’s high accuracy service, In *Proceedings of the 2022 International Technical Meeting of The Institute of Navigation*, 25-27 January 2022 Long Beach, CA, USA, 2022, 1246–1262, <https://doi.org/10.33012/2022.18261>
10. Fernandez-Hernandez I., Chamorro-Moreno A., Cancela-Diaz S., Calle-Calle J.D., Zoccarato P., Blonski D., Mozo A. Galileo High Accuracy Service: Initial definition and performance, *GPS Solutions*, 2022, 26 Article No. 65, Springer, 2022, <https://doi.org/10.1007/s10291-022-01247-x>
11. European Agency for the Space Programme (EUSPA). Galileo High Accuracy Service Signal-in-Space Interface Control Document (HAS SIS ICD) Issue 1.0, EUSPA, May 2022, [https://www.gsc-europa.eu/sites/default/files/sites/all/files/Galileo\\_HAS\\_SIS\\_ICD\\_v1.0.pdf](https://www.gsc-europa.eu/sites/default/files/sites/all/files/Galileo_HAS_SIS_ICD_v1.0.pdf)
12. European Agency for the Space Programme (EUSPA). Galileo - High Accuracy Service - Service Definition Document (Galileo HAS SDD) Issue 1.0, EUSPA, January 2023, [https://www.gsc-europa.eu/sites/default/files/sites/all/files/Galileo-HAS-SDD\\_v1.0.pdf](https://www.gsc-europa.eu/sites/default/files/sites/all/files/Galileo-HAS-SDD_v1.0.pdf)
13. Kiliszek D. GPS and Galileo Precise Point Positioning Performance with tropospheric estimation using different products: BRDM, RTS, HAS, and MGEX. *Remote Sens*. 2025, 17, 2080, <https://doi.org/10.3390/rs17122080>
14. Zoccarato P., Menzione F., Gioia C., Fortuny-Guasch J., Paonni M. Monitoring and data distribution of the galileo high-accuracy service system and user performance. *Eng. Proc*. 2025, 88, 13, <https://doi.org/10.3390/engproc2025088013>

15. Kerker V. GALILEO HAS overview, comparison with analogues, and assessment of perspective. *ISTCGCAP*. 2024, 100, 43–52, <https://doi.org/istcgcap2024.100.043>
16. Cappello G., Angrisano A., Ascione S., Del Pizzo S., Gioia C., Portelli G., Susi M., Gaglione S. Demonstrating Galileo Has in Single Point Positioning, In *Proceedings of the 2023 IEEE International Workshop on Metrology for Automotive (MetroAutomotive)*, Modena, Italy, 2023, 117–121, <https://doi.org/10.1109/MetroAutomotive57488.2023.10219138>
17. Yi D., Bisnath S., Naciri N., Javier De Blas F., Capua R. Galileo HAS: A Performance Assessment in Urban Driving Environments. *InsideGNSS*. November/December 2023, 56–65.
18. Cydejko J. GALILEO HAS – first performance tests during its initial phase of operation. *Aviation and Security Issues*. 2023, 3(1), 265–286, <https://doi.org/10.55676/asi.v3i1.46>
19. Smyrniaios M., Dilg W., Lutz K., Röttgers B., Furrner J. Performance analysis for the Galileo high-accuracy service and related work in the DLR Galileo competence center. *Eng. Proc.* 2025, 88, 2, <https://doi.org/10.3390/engproc2025088002>
20. Cucchi L., Damy S., Gioia C., Motella B., Paonni M. Galileo high accuracy service: Tests in Different operational conditions. *NAVIGATION: Journal of the Institute of Navigation*. 2024, 71(4), navi.665, <https://doi.org/10.33012/navi.665>
21. de Blas F. J., Vázquez J., Hernández C., Ostolaza J., Lagrasta S., Fernandez-Hernández I., Blonski D., The Galileo High Accuracy Service (HAS): A Pioneer Free-of-Charge Global Precise Positioning Service, In *Proceedings of the 36th International Technical Meeting of the Satellite Division of The Institute of Navigation (ION GNSS+ 2023)*, Denver, Colorado, September 2023, 449–468, <https://doi.org/10.33012/2023.19197>
22. de Blas F. J. Galileo High Accuracy Service (HAS): Status, architecture and roadmap. Available from: [https://www.gsc-europa.eu/sites/default/files/sites/all/files/2.HAS\\_DAYS\\_EUSPA\\_HAS\\_status-architecture-roadmap.pdf](https://www.gsc-europa.eu/sites/default/files/sites/all/files/2.HAS_DAYS_EUSPA_HAS_status-architecture-roadmap.pdf), (Accessed: 01.06.2025)
23. Fernandez-Hernandez I. Galileo High Accuracy Service (HAS). Available from: [https://www.unoosa.org/documents/pdf/icg/2024/WG-S\\_3rd\\_Workshop\\_Interoperability\\_PPP/3PITF2024\\_02.pdf](https://www.unoosa.org/documents/pdf/icg/2024/WG-S_3rd_Workshop_Interoperability_PPP/3PITF2024_02.pdf), (Accessed: 01.06.2025).
24. Angrisano A., Ascione S., Cappello G., Gioia C., Gaglione S. Application of “Galileo High Accuracy Service” on single-point positioning. *Sensors*, 2023, 23, 4223, <https://doi.org/10.3390/s23094223>
25. Bahadur B. Real-time single-frequency precise positioning with Galileo satellites. *Journal of Navigation*. 2022, 75(1), 124–140, <https://doi.org/10.1017/S037346332100076X>
26. Rapiński J., Tomaszewski D. Space State representation corrections as an aid in pseudolite positioning. *Sensors* 2019, 19, 4158. <https://doi.org/10.3390/s19194158>
27. Janicka J., Tomaszewski D., Rapinski J., Jagoda M., Rutkowska M. The Prediction of geocentric corrections during communication link outages in PPP. *Sensors* 2020, 20, 602, <https://doi.org/10.3390/s20030602>
28. Pelc-Mieczkowska R., Tomaszewski, D. Space state representation product evaluation in satellite position and receiver position domain. *Sensors* 2020, 20, 3791, <https://doi.org/10.3390/s20133791>
29. Yao W., Huang H., Ma X., Zhang Q., Yao Y., Lin X., Zhao Q., Huang Y. Multi-Global Navigation Satellite System (GNSS) real-time tropospheric delay retrieval based on state-space representation (SSR) products from different analysis centers, *Ann. Geophys.*, 2024, 42, 455–472, <https://doi.org/10.5194/angeo-42-455-2024>
30. Robustelli U., Pugliano G. Galileo single point positioning assessment including FOC satellites in eccentric orbits. *Remote Sens.* 2019, 11, 1555, <https://doi.org/10.3390/rs11131555>
31. Kwaśniak D. Ł., Cellmer S. Incorporating inter-system bias in single point positioning based on GPS, Galileo and BeiDou system. *Geomatics and Environmental Engineering*, 2021, 15(1), 97–109, <https://doi.org/10.7494/geom.2021.15.1.97>
32. Krasuski K., Ciećko A., Grunwald G., Wierzbicki D., Assessment of velocity accuracy of aircraft in the dynamic tests using GNSS sensors. *Facta Universitatis Series: Mechanical Engineering*, 2020, 18(2), 301–313, <https://doi.org/10.22190/FUME200302027K>
33. Grzegorzewski M. Navigating an aircraft by means of a position potential in three dimensional space, *Annual of Navigation*, 2005, 9, 1–111.
34. Mrozik M. Application of the SBAS positioning method in the aircraft approach procedure, PhD thesis. Silesian University of Technology, Gliwice, 2023, 1–147. (in Polish)
35. Matrice 350 RTK. Available from: <https://enterprise.dji.com/matrice-350-rtk>, (Accessed: 01.06.2025).
36. Savchuk S., Grzegorzewski M., Gołda P., Kerker V. Positioning using the precision GALILEO HAS Service. *Annual of Navigation*, 2024, 29, 60–68, <https://doi.org/10.36163/aon-2024-0007>
37. IGS State Space Representation (SSR) Format Version 1.00. Available from: [https://files.igs.org/pub/data/format/igs\\_ssr\\_v1.pdf](https://files.igs.org/pub/data/format/igs_ssr_v1.pdf), (Accessed: 01.06.2025).
38. RTKLIB website. Available from: <http://rtklib.com/>, (Accessed: 01.06.2025).
39. Prol F.S., Kirkko-Jaakkola M., Horst O., Malkamäki T., Zahidul H. Bhuiyan M., Kaasalainen S., Fernandez-Hernandez I. Enabling the Galileo high accuracy service with open-source software: integration of

- HASlib and RTKLIB, GPS Solutions, 2024, 28(71), <https://doi.org/10.1007/s10291-024-01617-7>
40. Takasu T. RTKLIB ver. 2.4.2 Manual, RTKLIB: An Open Source Program. Package for GNSS Positioning, 2013. Available from: [http://www.rtklib.com/prog/manual\\_2.4.2.pdf](http://www.rtklib.com/prog/manual_2.4.2.pdf), (Accessed: 01.06.2025).
  41. Specht M. Experimental studies on the relationship between HDOP and position error in the GPS system. *Metrology and Measurement Systems*. 2022, 29(1), 17-36, <https://doi.org/10.24425/mms.2022.138549>
  42. Antenna. Available from: <https://igs.org/wg/antenna/#files>, (Accessed: 01.06.2025).
  43. Emlid Studio website. Available from: <https://docs.emlid.com/emlid-studio/>, (Accessed: 01.06.2025).
  44. Elkhalea M.F., Hendy H., Kamel A., Abosekeen A., Noureldin A. Centralized measurement level fusion of GNSS and inertial sensors for robust positioning and navigation, *Sensors*, 2025, 25, 2804, <https://doi.org/10.3390/s25092804>
  45. RYKI reference station. Available from: <https://www.asgeupos.pl/ryki/>, (Accessed: 01.06.2025).
  46. Scilab webiste. Available from: <https://www.scilab.org/>, (Accessed: 01.06.2025).
  47. Specht C., Pawelski J., Smolarek L., Specht M., Dabrowski P. Assessment of the positioning accuracy of DGPS and EGNOS systems in the Bay of Gdansk using maritime dynamic measurements, *Journal of Navigation*, 2019, 72(3), 575–587, <https://doi.org/10.1017/s0373463318000838>
  48. Specht C., Mania M., Skóra M., Specht M. Accuracy of the GPS positioning system in the context of increasing the number of satellites in the constellation, *Polish Maritime Research*, 2015, 22, 9–14, <https://doi.org/10.1515/pomr-2015-0012>
  49. BOR1 reference station. Available from: <https://www.asgeupos.pl/bor1/>, (Accessed: 01.06.2025).
  50. Bogusz J., Brzeziński A., Godah W., Nastula J. Research on Earth rotation and geodynamics in Poland in 2019–2022, *Advances in Geodesy and Geoinformation*, 2023, 72(2), 1–42, <https://doi.org/10.24425/agg.2023.144593>
  51. Ayso E., Kahveci M. Performance assesment of GPS/Galileo enabled Single Point Positioning (SPP): a case study VACS station. In *Proceedings of the Deu International Symposium Series on Graduate Researches-2022 GeoScience*, December 8-9, 2022 Izmir, Türkiye, 1–9.
  52. Bosy J., Precise processing of satellite GPS observations in local networks located in mountain areas, *Wydawnictwo Akademii Rolniczej we Wrocławiu, Zeszyty Naukowe Akademii Rolniczej we Wrocławiu, Nr 522, Seria Rozprawy CCXXXIV*, Wrocław, 2005, 1–155. (in Polish)
  53. Kaloop M. R., Yigit C. O., El-Mowafy A., Bezcioglu M., Dindar A. A., Hu J. W. Evaluation of multi-GNSS high-rate relative positioning for monitoring dynamic structural movements in the urban environment, *Geomatics, Natural Hazards and Risk*, 2020, 11(1), 2239–2262, <https://doi.org/10.1080/19475705.2020.1836040>
  54. Gabryszuk J. Influence of elevation angle on RTN GNSS positioning with TPI NETPRO and VRSNET networks, *Infrastruktura i Ekologia Terenów Wiejskich*, 2016, 13/II/1, 299-309, <http://dx.medra.org/10.14597/infraeco.2016.2.1.021>. (in Polish)
  55. Marut G., Hadaś, T., Kazmierski, K. Bosy J. Affordable Real-Time PPP—Combining Low-Cost GNSS Receivers with Galileo HAS Corrections in Static, Pseudo-Kinematic, and UAV Experiments, *Remote Sens.*, 2024, 16, 4008, <https://doi.org/10.3390/rs16214008>
  56. Products IGS. Available from: <https://igs.org/products/#:~:text=IGS%20operational%20products%20include%20precise%20GNSS%20satellite%20ephemerides%2C,rates%2C%20length-of-day%29%2C%20and%20station%20and%20satellite%20clock%20solutions>, (Accessed: 01.06.2025).
  57. CSRS-PPP. Available from: <https://webapp.csrscs.nrcan-rncan.gc.ca/geod/tools-outils/ppp.php>, (Accessed: 01.06.2025).
  58. Abdallah A., Agag T. Reliability of CSRS-PPP for validating the Egyptian geodetic CORS networks, *Artificial Satellites*, 2022, 57(1), 58–76, <https://doi.org/10.2478/arsa-2022-0004>.
  59. CSRS-PPP Updates and Information. Available from: <https://webapp.csrscs-scrcs.nrcan-rncan.gc.ca/geod/tools-outils/ppp-info.php?locale=en>, (Accessed: 01.06.2025).
  60. Krasuski K., Savchuk S. Accuracy Assessment of Aircraft Positioning Using the Dual-Frequency GPS Code Observations in Aviation. *Communications - Scientific Letters of the University of Zilina*, 2020, 22(2), 23–30, <https://doi.org/10.26552/com.C.2020.2.23-30>